Tumor Biol.
DOI 10.1007/s13277-013-1396-5

RESEARCH ARTICLE

Anti-hepatoma cells function of luteolin through inducing apoptosis and cell cycle arrest

Shixiong Ding · Airong Hu · Yaoren Hu · Jianbo Ma · Pengjian Weng · Jinhua Dai

Received: 24 September 2013 / Accepted: 5 November 2013

Abstract The aim of this study is to explore the apoptotic induction and cell cycle arrest function of luteolin on the liver cancer cells and the related mechanism. The liver cancer cell line SMMC-7721, BEL-7402, and normal liver cells HL-7702 were treated with different concentrations of luteolin. Cell proliferation ability was tested. Morphological changes of the apoptotic cells were observed under inverted fluorescence microscope after Hoechst33342 staining. We investigated the effect of luteolin on cell cycling and apoptosis with flow cytometry. The mitochondrial membrane potential changes were analyzed after JC-1 staining. Caspases-3 and Bcl-2 family proteins expression were analyzed by real-time PCR. Cell proliferation of SMMC-7721 and BEL-7402 were inhibited by luteolin, and the inhibition was dose–time-dependent. Luteolin could arrest the cells at G1/S stage, reduce mitochondrial membrane potential, and induce higher apoptosis rate and the typical apoptotic morphological changes of the liver carcinoma cells. Q-RT-PCR results also showed that luteolin increased Bax and caspase-3 expression significantly and upregulated Bcl-2 expression in a dose-dependent manner in liver carcinoma cells. However, the normal liver cells HL-7702 was almost not affected by luteolin treatment. Luteolin can inhibit SMMC-7721 and BEL-7402 cell proliferation in a time- and dose-dependent manner. And the mechanism maybe through arresting cell cycle at phase G1/S, enhancing Bax level, reducing anti-apoptotic protein Bcl-2 level, resulting in activating caspase-3 enzyme and decrease of mitochondrial membrane potential, and finally leading to cell apoptosis.

Keywords Luteolin · Liver cancer · Cell apoptosis · Cell cycle

Introduction

Liver cancer represents one of the most common neoplasms worldwide. It is the second and sixth leading cause of cancer-related death in males and females, respectively [1]. Currently, surgical resection and local ablative therapies are adopted frequently when liver transplantation is not accessible, and recurrence is the main reason of death after surgical treatment for this cancer. So finding effective natural medicine which has anti-liver carcinoma effect is of great significance undoubtedly.

Many researchers have reported that flavonoids can be used as effective natural inhibitor on cancer initiation and progression. Recently, luteolin (3′,4′,5,7-tetrahydroxyflavone), which was extracted from radix arnebiae seu lithospermi root, known as common dietary flavonoid and found in fruits, vegetables, medicinal herbs [2], has been found possessing a potent antitumor activity in several studies [3–5]. It displays a significant effect on killing malignant cells even at a low dosage. But the functions and the detailed mechanism of luteolin on human liver cancer were not reported till now. This study focused on the cell apoptotic effect and cell cycle arrest of luteolin on liver cancer cells and the detailed mechanism.

S. Ding · J. Ma · P. Weng · J. Dai
Department of Laboratory Medicine, The Affiliated Ningbo No.2 Hospital, College of Medicine, Ningbo University, Ningbo, Zhejiang 315010, China

A. Hu · Y. Hu (✉)
The Affiliated Ningbo No.2 Hospital, College of Medicine, Ningbo University, Ningbo, Zhejiang 315010, China
e-mail: yaoren_hu@126.com

Y. Hu
e-mail: Hu510@126.com

A. Hu · Y. Hu
Institute of Liver Disease, Ningbo, Zhejiang 315010, China

Published online: 28 November 2013

The experimental materials and methods

Cell culture

Liver carcinoma cell lines SMMC-7721 and BEL-7402 were purchased from ATCC (Manassas, VA, USA), and normal liver cell line HL-7702 was bought from Shanghai cell bank of Chinese academy of sciences (Shanghai, China). All the cell lines identities were mycoplasma-free and were cultured in Dulbecco modified Eagle medium (DMEM, Gibco, USA) supplemented with 10 % heat-inactivated fetal calf serum (FCS, Gibco, USA) at 37 °C and 5 % CO_2 atmosphere.

Luteolin liquids preparation

One microgram luteolin (from Sigma) was dissolved with l00-μl DMSO, and stored at −20 °C. This stock solution was diluted with DMEM and prepared with the cell culture medium containing different concentrations of luteolin. This medium was filtered and stored under 4 °C in dark condition.

Cell proliferation assay

Cell titer 96 ® AQ_{ueous} nonradioactive cell proliferation assay was applied to determine cell proliferation ability. Briefly, the SMMC-7721, BEL-7402, and normal liver cells HL-7702 were collected at logarithmic phase, diluted into 5×10^4 cells/mL with DMEM containing 10 % fetal calf serum, seeded into 96-well flat-bottom plates, 100 μl/well, and incubated at 37 °C and 5 % CO_2 atmosphere for 24 h. Then cells were cultured in 100-μl DMEM medium with different concentration of luteolin (0, 12.5,25, 50, 75, and 100 μM) and 10 % fetal calf serum, at 37 °C and 5 % CO_2 condition for 0,1, 2, and 3 days. After that, 20-μl Cell titer 96 ® AQ_{ueous} nonradioactive cell proliferation assay reagent was added (Promega, USA) into each well, then incubated for 3 h. The absorption values at 490 nm were examined with the automatic enzyme-linked immunosorbent assay plate reader (BMG POLARstar Omega, BMG Labtech, Germany). The inhibition rate was calculated according to the following formula:

$$\text{Inhibition rate} = (\text{OD value of control group} - \text{OD value of test group})/\text{OD value of control group} \times 100\%.$$

Mitochondrial membrane potential assessment

Mitochondria play an important role in cell apoptosis, and mitochondrial membrane potential decline is an earlier event of the apoptosis. 5,5′,6,6′-tetrachloro-1,1′,3,3′-tetraethylbenzimi-dazolylcarbocyanine iodide (JC-1) is an effective reagent for mitochondrial membrane potential detection. When the mitochondrial membrane potential is lower, JC-1 will exist in monomer, and the cells show green fluorescence. On the contrary, the dimer forms when the mitochondrial membrane potential is higher, and the cells show red fluorescence [6]. In this study, to measure the mitochondrial membrane potential for apoptosis analysis, JC-1 staining was performed with Accuri's JC-1 mitochondrial potential assay kit (Invitrogen, USA) according to the protocol after the liver cancer cells SMMC-7721 and BEL-7402 were treated with 0 or 50 μM luteolin for 24 h.

Nucleus morphological changes observation

The fastest way to detect apoptosis is the observation of nucleus morphology variations using Hoechst staining. In this research, the Hoechst 33342 stain was applied to distinguish the apoptotic cell nucleus. Briefly, cells in logarithmic growth phase were seeded into the 6-well plates at 4×10^4 cells/well. After pre-incubation for 12 h under normal condition, cells were cultured with luteolin (0, 25, 50 μM) and 10 % fetal calf serum in DMEM. Each treatment was tested in triplicate. After 24 h, cells were washed with PBS twice, fixed with 1 ml of 4 % paraformaldehyde at 4 °C for 10 min. Then the cells were washed with PBS for three times, dyed with Hoechst 33342 (Sigma, USA, 5 μg/ml in PBS) for 10 min at the room temperature in dark condition, and observed under an inverted fluorescence microscope immediately after washing with PBS three times. Dead cells will not be dyed by Hoechst staining. The healthy cells will show large oval-shaped body with uniform fluorescence in nuclei. When cell apoptosis happens, nuclear morphological changes, such as blue fluorescent stained compact particulates, can be seen in the nucleus. The cells with three or more than three fluorescent DNA fragments are identified as apoptosis cells.

Assessment of apoptosis

The cells at logarithmic growth phase were seeded into 6-well plates at 4×10^5 cells/well, incubated under 37 °C 5 % CO_2 condition for 24 h. The culture medium was changed with 2-ml DMEM, which contain 0 or 50 μM luteolin and 10 % fetal calf serum, and cultured at 37 °C 5 % CO_2 atmosphere for 24 h.

Table 1 The primer sequences of GAPDH, Bcl-2, Bax, and caspase-3

Primer name	Primer sequences	Annealing condition
GAPDH-F	TGAAGGTCGGAGTCAACGG	60 °C, 60 s
GAPDH-R	CTGGAAGATGGTGATGGGATT	
BC12-F	GGGTGGGAGGGAGGAAGAAT	60 °C, 60 s
BCL2-R	TTCGCAGAGGCATCACATCG	
BAX-F	CTCACCGCCTCACTCACCAT	60 °C, 60 s
BAX-R	TGTGTCCCGAAGGAGGTTTATT	
Caspase3-F	GAGTAGATGGTTTGAGCCTGAG	60 °C, 60 s
Caspase3-R	TGCCTCACCACCTTTAGAAC	

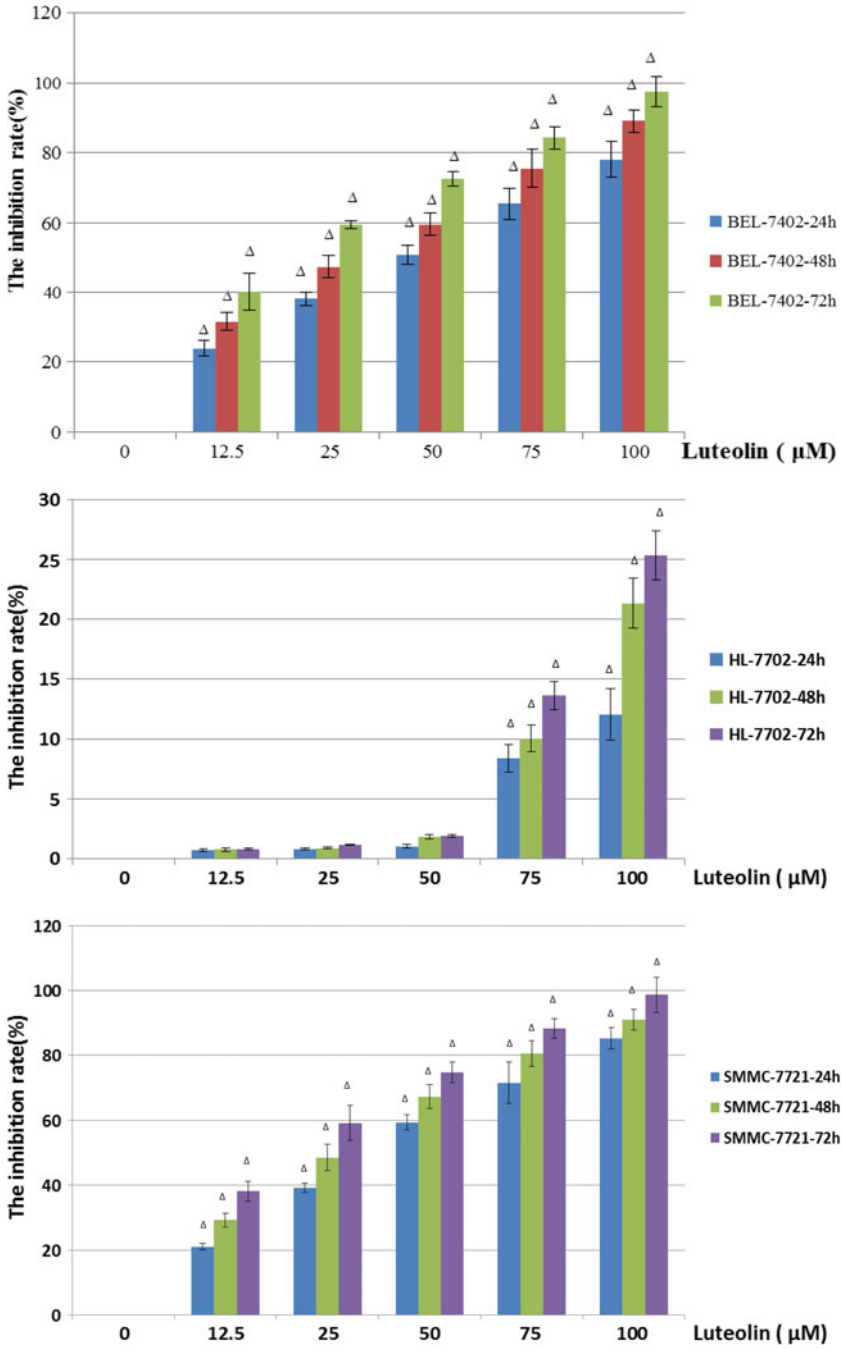

Fig. 1 The inhibition of SMMC-7721, BEL-7402, and HL-7702 cell proliferation treated with luteolin for 24, 48, or 72 h ($\bar{x} \pm s$, $n=3$). Note: Compared with 0 μM luteolin treated group, respectively. *White triangle* $P<0.01$

Each treatment was tested in triplicate. The cells were harvested after digestion with pancreatic enzymes, washed with PBS three times, and double stained with phycoerythrin-conjugated Annexin V and 7AAD according to the manufacturer's instructions (BD Bioscience, San Jose, CA). Twenty thousand events were collected for each sample using a Becton Dickinson FACScan (BD Bioscience, San Jose, CA). Data were analyzed with FlowJo software (Tree Star, San Carlos, CA). Both early apoptotic (Annexin V positive, 7-AAD negative) and late apoptotic (Annexin V positive, 7-AAD positive) cells were included in cell apoptosis.

The cell cycle analysis

The cells at logarithmic growth phase were seeded into 6-well plates at 4×10^5 cells/well, incubated at 37 °C with 5 % CO_2 for 24 h. The medium was changed with 2-ml DMEM containing 0 or 4 μM luteolin and 10 % fetal calf serum, and cultured at 37 °C 5 % CO_2 atmosphere for 24 h. The cells were harvested after digestion with pancreatic enzymes, washed with cold PBS three times, and fixed with ice-cold 70 % ethanol at −20 °C overnight. After centrifuged for 5 min at 1,500 rpm, the cells were re-suspended in 5-mL fluorescence-

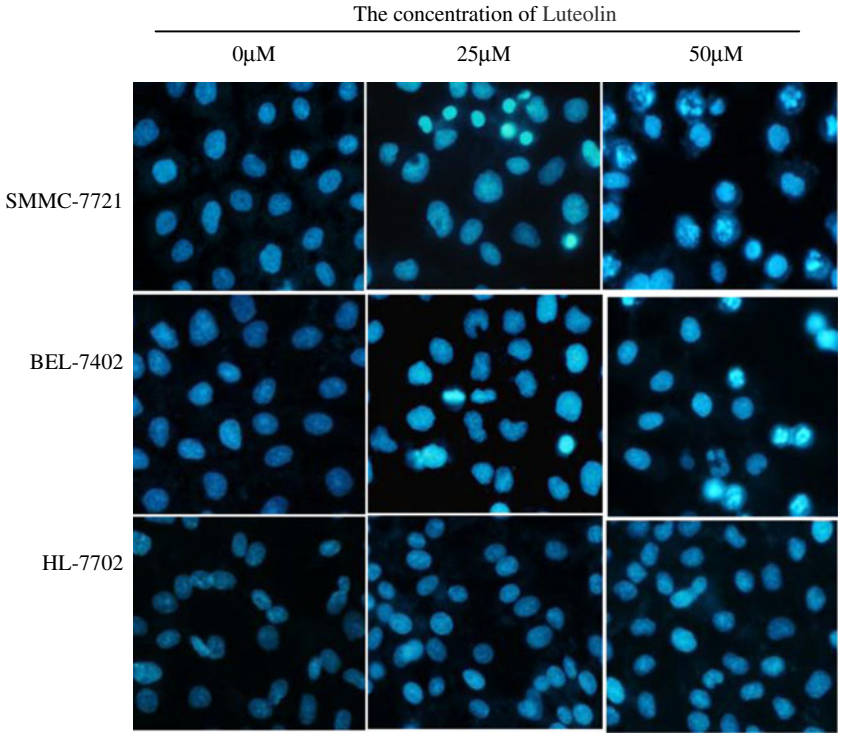

Fig. 2 The morphology changes of the cell nucleus in cell lines HL-7702, SMMC-7721, and BEL-7402 induced by luteolin was observed under the inverted fluorescence microscope after Hoechst staining (×400)

activated cell sorting washing medium (3 % FCS/PBS) and centrifuged again. Cell pellets were re-suspended in 0.5 mL of PI/RNase staining buffer (BD Pharmingen™, USA) and incubated at room temperature for 30 min. DNA content in each cell was examined by flow cytometer (BD Bioscience, San Jose, CA). The percentage of cell population of G1, S, and G2 phases was determined by FlowJo software (Tree Star, San Carlos, CA).

Bcl-2, Bax, and caspase-3 mRNA expression level examination

The SMMC-7721, BEL-7402, and HL-7702 cells were collected after 0 or 50-μM luteolin treatment for 24 h; total RNA was extracted from the cells using TRIzol™ reagent (Invitrogen Company, USA). Briefly, 1-mL Trizol was added to PBS washed cells, mixed by pipetting until the solutions were transparent and clear, incubated in the room temperature for 5 min, added 200-μl chloroform and mixed well, incubated in the room temperature for 3 min, and centrifuged for 15 min at 12,000 rpm 4 °C condition. The supernatant was transferred into a 1.5-mL centrifuge tube with 500 μL isopropanol, mixed well, incubated for 10 min at the room temperature, and centrifuged at 12,000 rpm for 15 min at 4 °C. The supernatant was discarded, adding 1 mL 75 % ethanol to clean the RNA sediment, centrifuged for 5 min at 12,000 rpm 4 °C condition. The supernatant was discarded, air dried for 10 min, and dissolved the RNA pellet in 50 μL RNAse free water. RNA was quantified with Nano drop (Thermo fisher), and its integrity was detected by agarose gel electrophoresis. Then the RNAs were reverse-transcripted with the SuperScript® III First-Strand Synthesis System (Invitrogen™). One microliter RT product was used for subsequent reverse transcription real-time PCR (Q-RT-PCR) with the final concentration of PCR reaction being 2.5× real master mix/20× SYBR solution mixture 9 μL, upstream and downstream primers 2 μL (100 nmol/L, produced by Sangon Biotech company Shanghai, China). The primer sequences were listed in Table 1. The ddH_2O was added to reach the total volume of 20 μL. The Ct value of each cell was recorded, and the data were analyzed by the comparative Delta-delta Ct method.

Statistical analysis

All data were analyzed by SPSS16.0 software (SPSS Inc., Chicago, IL), and presented as mean ± SD. Kruskal–Wallis test

Table 2 The total apoptosis rate including the early and late apoptotic cells of HL-7702, SMMC-7721, and BEL-7402 cell lines after luteolin treatment

Cell line	The apoptotic rate (%)	
	0 μM luteolin treated	50 μM luteolin treated
SMMC-7721	11.06±3.22	58.18±2.11*
BEL-7402	6.58±0.46	37.70±3.04*
HL-7702	6.94±0.27	7.79±0.54

Compared with 0 μM luteolin treated group respectively, *$P<0.01$

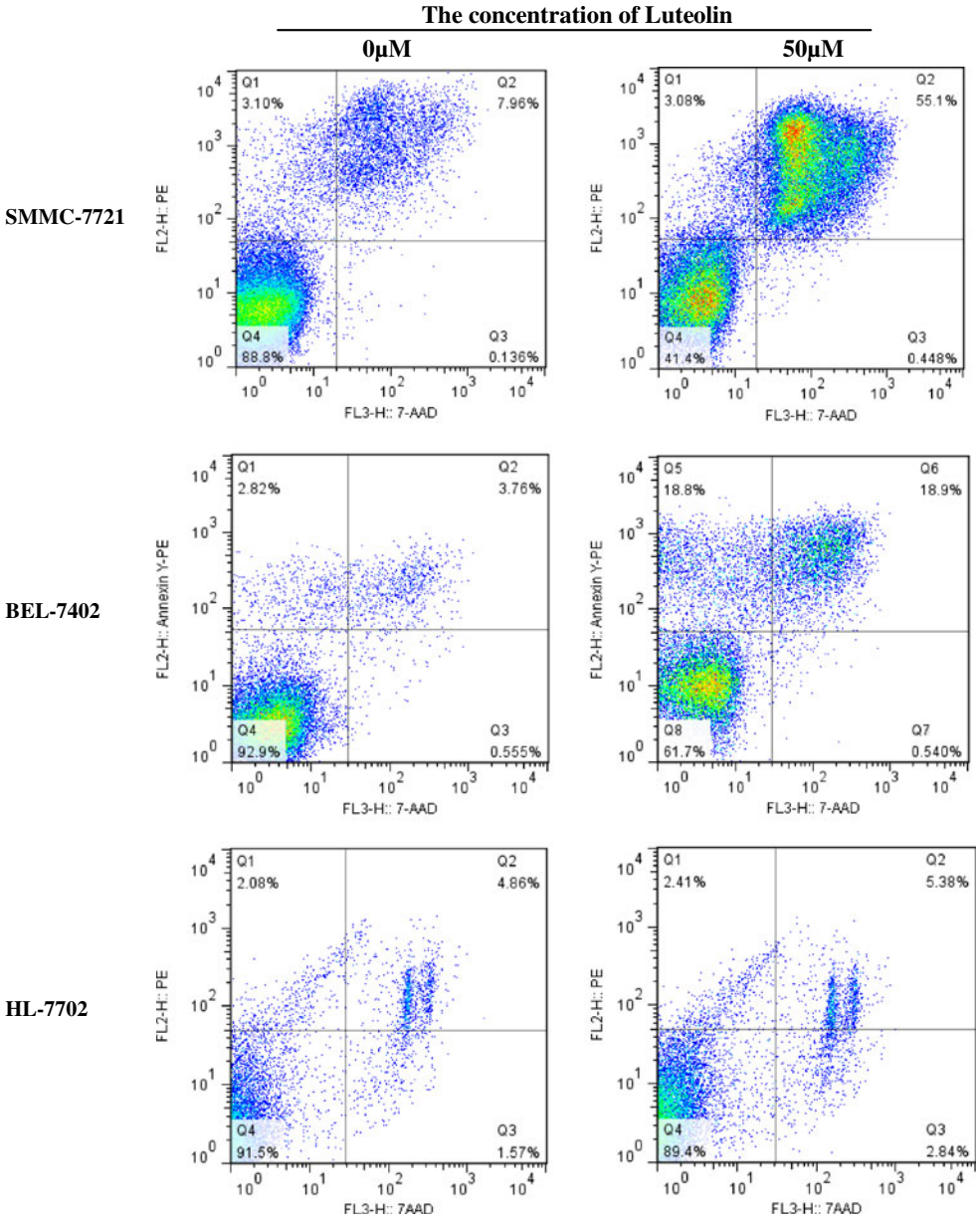

Fig. 3 Apoptosis assessment by flow cytometry after cells treated with luteolin (0 or 50 μM) for 24 h and dyed by Annexin V/7-AAD double staining

was used for multiple group comparisons followed by Wilcoxon rank sum test including Bonferroni adjustment for comparison between two groups. All tests performed were two-sided. $P<0.05$ was considered significantly different.

Results

Luteolin-inhibited liver cancer cells proliferation

The cell proliferation data showed in Fig. 1; the liver cancer cells proliferation was inhibited by different concentrations of luteolin after 24, 48, or 72-h treatment, and the inhibition effect was dose- and time-dependent. However, no significant inhibition was observed in the normal liver cell line HL-7702 treated with 12.5, 25, and 50 μM luteolin compared to 0 μM luteolin-treated group ($P>0.05$). When the concentration of luteolin reached 75 μM, proliferation of HL-7702 cells was inhibited in a time- and dose-dependent manner ($P<0.05$).

Luteolin-induced morphological changes of liver cancer cell nucleus

The cell nuclei of SMMC-7721, BEL-7402 dyed by Hoechst33342 are uniform, round or oval, chromatin distribution uniformity (shown in Fig. 2). After luteolin treatment, more cells appeared characteristics of apoptosis with the changes of nuclear morphology such as chromatin condensation, round cell karyorrhexis particles formation, the particle shape distribution, the lobulated nuclear fragmentation, and

Table 3 The cell cycles of the cell lines which were treated with luteolin

Cell lines	Cell phase	Percentage of cell phase (%)	
		0 μM luteolin	50 μM luteolin
SMMC-7721	G1	59.86±1.07 %	66.05±2.06 % *
	S	21.43±0.58 %	30.33±1.12 % *
	G2	14.75±0.75 %	3.24±0.39 % **
BEL-7402	G1	54.81±2.33 %	63.14±2.17 % *
	S	20.72±1.09 %	31.92±1.16 % **
	G2	14.78±0.67 %	4.91±0.54 % **
HL-7702	G1	75.2±2.08 %	76.26±3.21 %
	S	21.35±0.62 %	20.23±1.14 %
	G2	3.32±0.47 %	2.91±0.23 %

Compared with 0 μM luteolin treatment group, *$P<0.05$, **$P<0.01$

bright blue karyopyknosis. The morphology of the cell nucleus in normal cells HL-7702 treated by luteolin was not changed as much as the liver cancer cell.

Luteolin-induced apoptosis of liver cancer cells

The liver cancer cells SMMC-7721 and BEL-7402 and the normal cells HL-7702 were treated with 50 μM luteolin. The apoptosis rates were examined by flow cytometry after cells were dyed with Annexin V-PE and 7-AAD. Data showed in Table 2 and Fig. 3 the total apoptosis rates (including early apoptotic cells and later stage of apoptosis) for SMMC-7721 and BEL-7402 cells reached to 58.18±2.11 and 37.7±3.04 % after 50 μM luteolin treatment, which is significantly different from the normal liver cells and 0 μM luteolin-treated group,

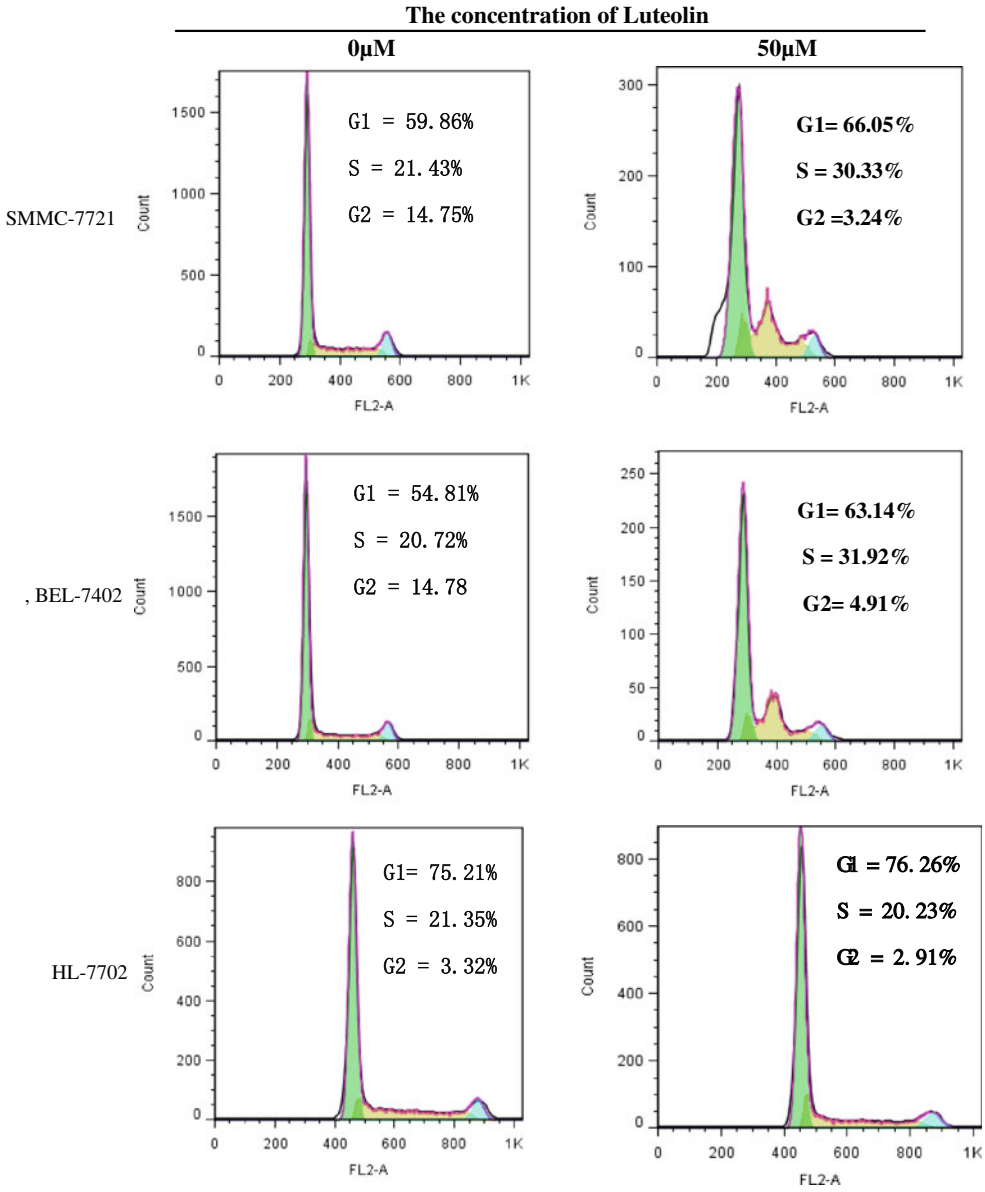

Fig. 4 The cell cycles of liver carcinoma cells SMMC-7721, BEL-7402, and normal liver cells HL-7702 treated with 0 or 50 μM of luteolin for 24 h

($P<0.01$). The results demonstrated that luteolin had a dose-dependent apoptosis inducing function on liver cancer cells including SMMC-7721 and BEL-7402, but showed a very slight apoptosis inducing function to normal liver cells HL-7702.

The cell cycles of liver carcinoma cells were changed by luteolin

Liver carcinoma cells SMMC-7721 and BEL-7402 were treated with 0 or 50 μM of luteolin for 24 h, and the cell cycle were evaluated with flow cytometry. The data showed in Table 3 and Fig. 4 that luteolin arrested cell cycle progression in the G1/S phase and prevented entry into G2 phase ($P<0.01$). But the cell cycle of normal liver cells was almost not influenced by luteolin treatment, ($P>0.05$).

Reduced mitochondrial membrane potential of liver cancer cells after luteolin treatment

JC-1 can selectively enter into mitochondria and reversibly change color from red to green following the decline of membrane potential [7]. If apoptosis induced by luteolin is through the mitochondrial pathway, the mitochondrial membrane integrity will be damaged at the early stage of cell apoptosis; the membrane potential should be reduced, and the JC-1 will exist mainly in a monomeric form in the cells, and emit green fluorescence. In this study, the data showed in Fig. 5 suggested that, compared with 0 μM luteolin-treated group, mitochondria membrane potentials of SMMC-7721 and BEL-7402 cells were decreased after 50 μM luteolin treatment, so cell apoptosis induced by luteolin may be associated with the mitochondrial membrane potential decline.

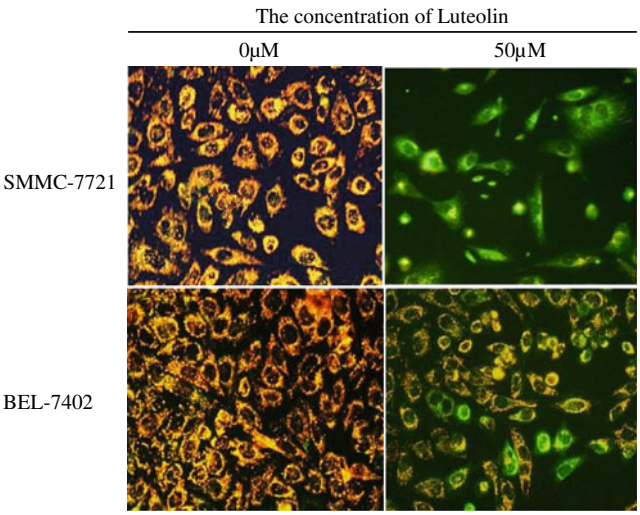

Fig. 5 The mitochondria membrane potentials decrease of SMMC-7721 and BEL-7402 cells after luteolin treatment

Expression of multiple proteins in the mitochondria signaling pathways changed after luteolin treatment

Many evidences showed that the caspase cascade and Bcl-2 protein family play an important role in the mitochondria-mediated cell apoptosis [8], so we studied the effect of luteolin on caspases and Bcl-2 family in liver carcinoma and the normal cell lines SMMC-7721, BEL-7402, and HL-7702 by Q-RT-PCR. Q-RT-PCR results were listed in Fig. 6. Data showed that the mRNA levels of Bax, Bcl-2, and caspase-3 of the cell lines SMMC-7721 and BEL-7402 were changed after 50 μM luteolin treatment, but the luteolin had no significant effect on HL-7702 cells ($P>0.05$).

Discussion

Cell apoptosis is an important mechanism for cell differentiation, body development, physiological, and pathological death. It is an actively programmed cell death process for maintaining a stable internal environment. Abnormal cell apoptosis is an important etiology for most malignant tumors, and searching for effective drugs to induce tumor cell apoptosis has become the target in the cancer therapy and studies.

Mitochondrial apoptosis pathway is also known as an endogenous apoptosis pathway. It is the major target of anticancer drugs in inducing tumor cell apoptosis [9, 10]. In this pathway, some stimulators which can result in the DNA damage will trigger the apoptotic process, and a series of genes including mammalian Bcl-2 and BAX will be activated by proteolysis or dephosphorylation of the proteins. Bcl-2 and BAX belong to the Bcl-2 family; they are key members of apoptosis-related genes in mitochondrial apoptosis pathway. Bcl-2 proteins are able to promote or inhibit apoptosis by direct action. BAX forms the pore on the cell, while Bcl-2 inhibits its formation. BAX promotes apoptosis by competing with Bcl-2 proper. Therefore, the expression of BAX, Bcl-2, and the ratio of them were selected as apoptosis markers for antitumor medicine examination in many studies [11]. When

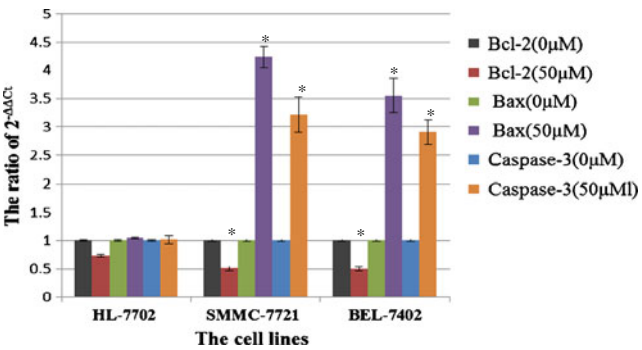

Fig. 6 The effect of luteolin on the expression of Bcl-2, Bax, and caspase-3 mRNA in HL-7702, SMMC-7721, and BEL-7402 cell lines ($\bar{x} \pm s$, $n=3$). Note: Compared with 0 μM luteolin treatment, $^*P<0.01$

the balance of Bcl-2 and Bax is broken, and Bax is in a dominant position, caspase-3 will be upregulated; the mitochondrial membrane potential will be downregulated. Then apoptosis signaling molecules such as cytochrome C will enter into the cytoplasm, activate the caspase, and lead to cell apoptosis [8].

Accumulating lines of evidence showed that luteolin, a polyphenolic compound, has several beneficial biological effects, including anti-inflammation [12], neuroprotection [13], antioxidant, suppressing tumor invasion and metastasis [14]. But the studies about its anti-liver carcinoma effects and the related mechanisms were rarely conducted.

To clarify the anti-liver cancer function of luteolin and its related mechanism, a series of studies were performed in this study. Data showed that luteolin could inhibit the growth of liver cancer cells in dose- and time-dependent manner. It could decrease the mitochondrial membrane potential of liver cancer cells through improving the level of apoptosis precursor protein Bax, downregulating antiapoptotic protein Bcl-2, and increasing Bax/Bcl-2 ratio, activate the caspase-3 cascade, and result in cell apoptosis. At the same time, luteolin arrested the liver cancer cells at stage G1/S, preventing the cells entry into G2 phase. The good news is that the cell apoptosis rate, cell cycle, the shape of cell nucleus, and the mRNA levels of caspase-3, Bcl-2, and Bax of normal liver cells were not changed significantly when the dosage of luteolin is not more than 75 μM.

In conclusion, our findings highlighted a novel mechanism for luteolin to anti-liver carcinoma, and supplied a certain reference value for the application of luteolin in clinical therapy of liver carcinoma in the future.

Conflicts of interest None

References

1. Khare S, Zhang Q, Ibdah JA. Epigenetics of hepatocellular carcinoma: role of microRNA. World J Gastroenterol. 2013;19(33):5439–45.
2. Pratheeshkumar P, Son Y-O, Budhraja A, et al. Luteolin inhibits human prostate tumor growth by suppressing vascular endothelial growth factor receptor 2-mediated angiogenesis. PLoS One. 2012;7(12):e52279.
3. Fu J, Chen D, Zhao B, et al. Luteolin induces carcinoma cell apoptosis through binding Hsp90 to suppress constitutive activation of STAT3. PLoS One. 2012;7(11):e49194.
4. Ju W, Wang X, Shi H, et al. A critical role of luteolin-induced reactive oxygen species in blockage of tumor necrosis factor-activated nuclear factor-kappaB pathway and sensitization of apoptosis in lung cancer cells. Mol Pharmacol. 2007;71:1381–8.
5. Cai X, Ye T, Liu C, et al. Luteolin-induced G2 phase cell cycle arrest and apoptosis on non-small cell lung cancer cells. Toxicol In Vitro. 2011;25(7):1385–91.
6. Salvioli S, Ardizzoni A, Franceschi C, et al. JC-1, but not DiOC6(3) or rhodamine 123, is a reliable fluorescent probe to assess delta psi changes in intact cells/implications for studies on mitochondrial functionality during apoptosis. FEBS Lett. 1997;411(1):77–82.
7. Elumalai P, Gunadharini DN, Senthilkumar K, et al. Induction of apoptosis in human breast cancer cells by nimbolide through extrinsic and intrinsic pathway. Toxicol Lett. 2012;215(2):131–42.
8. Leibowitz B, Yu J. Mitochondrial signaling in cell death via the Bcl-2 family. Cancer Biol Ther. 2010;9(6):417–22.
9. Das S, Das J, Samadder A, et al. Efficacy of PLGA-loaded apigenin nanoparticles in Benzo[a] pyrene and ultraviolet B-induced skin cancer of mice: mitochondria mediated apoptotic signaling cascades. Food Chem Toxicol. 2013;62C:670–80.
10. Qin R, Shen H, Cao Y, et al. Tetrandrine induces mitochondria-mediated apoptosis in human gastric cancer BGC-823 cells. PLoS One. 2013;8(10):e76486.
11. Kim SM, Kim YG, Park JW, et al. The effects of dexamethasone on the apoptosis and osteogenic differentiation of human periodontal ligament cells. J Periodontal Implant Sci. 2013;43(4):168–76.
12. Wu W, Li D, Zong Y, et al. Luteolin inhibits inflammatory responses via p38/MK2/TTP-mediated mRNA stability. Molecules. 2013;18(7):8083–94.
13. Nazari QA, Kume T, Takada-Takatori Y, et al. Protective effect of luteolin on an oxidative-stress model induced by microinjection of sodium nitroprusside in mice. J Pharmacol Sci. 2013;122(2):109–17.
14. Cheng WY, Chiao MT, Liang YJ, et al. Luteolin inhibits migration of human glioblastoma U-87 MG and T98G cells through downregulation of Cdc42 expression and PI3K/AKT activity. Mol Biol Rep. 2013;40(9):5315–26.